Ditopic halogen bonding with bipyrimidines and activated pyrimidines

Chideraa I. Nwachukwu[a], Leanna J. Patton[a], Nathan P. Bowling[b] and Eric Bosch[a]*

[a]Chemistry Department, Missouri State University, 901 South National Avenue, Springfield, Missouri, 65897, USA

[b]Department of Chemistry, University of Wisconsin-Stevens Point, 2001 Fourth Avenue, Stevens Point, WI, 54481, USA

Correspondence email: ericbosch@missouristate.edu

Funding information National Science Foundation, Directorate for Mathematical and Physical Sciences (grant No. 1903593).

Synopsis The role of activated pyrimidines and bipyrimidines as ditopic halogen bond acceptors is demonstrated.

Abstract The potential of pyrimidines to serve as ditopic halogen bond acceptors is explored. The halogen bonded cocrystals formed from solutions of either 5,5'-bipyrimidine or 1,2-bis(5-pyrimidyl) ethyne and 2 molar equivalents of 1,3-diiodotetrafluorobenzene have a 1:1 composition. Each pyrimidine moiety acts as a single halogen bond acceptor and the bipyrimidines as ditopic halogen bond acceptors. In contrast, the activated pyrimidines 2- and 5-(N,N-dimethylamino-phenylethynyl)pyrimidine are ditopic halogen bond acceptors and 1:1 halogen bonded cocrystals are formed from 1:1 mixtures of each of the activated pyrimidines and either 1,2- or 1,3-diiodotetrafluorobenzene. A 1:1 cocrystal was also formed between 2-(N,N-dimethylamino-phenylethynyl)pyrimidine and 1,4-diiodotetrafluorobenzene while a 2:1 cocrystal was formed between 5-(N,N-dimethylaminophenylethynyl)pyrimidine and 1,4-diiodotetrafluorobenzene.

Keywords: Pyrimidine halogen bond acceptor, diiodotetrafluorobenzene, ditopic halogen bond acceptor, supramolecular polymer.

1. Introduction

Halogen bonding, a well-established non-covalent interaction has been applied to a wide variety of areas, highlighting it's importance in chemistry. Most notably is the application of halogen bonding in crystal engineering, supramolecular chemistry and a variety of other fields that involve the design of functional molecules (Cavallo, *et al*., 2016; Gilday, *et al*., 2015). Pyridines are one of the most common aromatic halogen bond acceptors, while bipyridines have been demonstrated as effective ditopic halogen bond acceptors that allow the design of extended halogen bonded networks as well as discreet multicomponent complexes. Surprisingly, pyrimidines have rarely been employed as ditopic halogen bond acceptors. A search of the Cambridge Structural Database version 5.40 update 3 (Groom, *et al*., 2016) using ConQuest Version 2.04 (Bruno, *et al*, 2002) for pyrimidines with at least one N---I interaction with N---I distance less than the sum of the van der Waals radii and the angle between the N---I bond and the pyrimidine ring greater than 135° yielded 15 hits. Of these 9 corresponded to structures of single small molecules that included both a pyrimidine and an iodine atom and a C-I---N interaction. One of these structures features a halogen bond to an iodine molecule (van der Helm, 1973). The remaining 5 correspond to N---I interactions between different halogen bond donor and halogen bond acceptor molecules. Two structures feature bifurcated halogen bonds between 4,4',6,6'-tetramethyl-2,2'-bipyrimidine and 1,3-diiodo-tetrafluorobenzene (Ji, et al., 2011) and 1,4-diiodo-tetrafluorobenzene (Ji, et al., 2013) in which each pyrimidine molecule forms two weak bifurcated halogen bonds with N---I distances between 3.313 and 3.462 Å, 94-98% of the sum of the van der Waals radii. Interestingly, a 3:1 cocrystal formed between 1,3,5-trifluoro-2,4,6-triiodobenzene and 4,4',6,6'-tetramethyl-2,2'-bipyrimidine in which 3 of the 4 bipyrimidine N atoms form halogen bonds with four unique N---I distances between 3.089 and 3.463 Å and C-I---N angles between 137.245 and 177.919° (Ji, et al., 2013). In this report we first explore the halogen bonding of 5,5'-bipyrimidine **(2)** and 1,2-bis(5-pyrimidyl)ethyne **(1)** with 1,3-diiodotetrafluorobenzene and then demonstrate the role of activated pyrimidines, 5-(4-N,N-dimethylaminophenylethynyl)pyrimidine **(3)** and 2-(4-N,N-dimethylaminophenylethynyl)pyrimidine **(4)**, as ditopic halogen bond acceptors on cocrystallization with 1,2-, 1,3-, and 1,4-diiodotetrafluorobenzene.

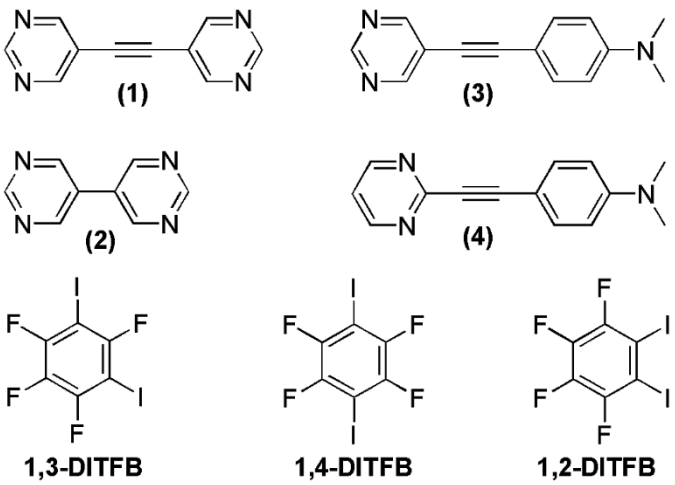

2. Experimental

2.1. Chemicals

1,2-Bis(5-pyrimidyl)ethyne, (**1**), (Georgiev, *et al*, 2004) and 5,5'-bipyrimidine, (**2**), (Barnes & Bosch, 2005) were available from previous studies. 1,2,3,5-Tetrafluoro-4,6-diiodobenzene was purchased from Synquest while 1,2,3,4-tetrafluoro-5,6-diiodobenzene and 1,2,4,5-tetrafluoro-3,6-diiodobenzene were purchased from Matrix Scientific. The activated pyrimidines, (**3**) and (**4**), were synthesized according to the synthetic scheme shown in Figure 1.

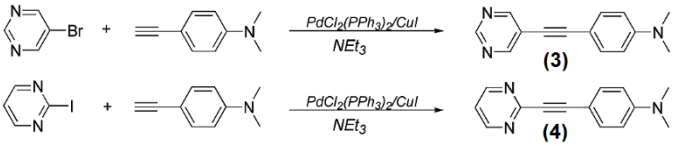

Figure 1 The preparation of 5-(4-N,N-dimethylaminophenylethynyl)pyrimidine **(3)** and 2-(4-N,N-dimethylaminophenylethynyl)pyrimidine **(4)** using the standard Sonogashira coupling.

2.1.1. Synthesis of 5-(4-N,N-dimethylaminophenylethynyl)pyrimidine, (3)

5-Bromopyrimidine (0.22 g, 1.4 mmol), $PdCl_2(PPh_3)_2$ (24 mg, 0.03 mmol), CuI (15 mg, 0.07 mmol) and 4-ethynyl-N,N'-dimethylaniline (0.19, 1.3 mmol) were added to a mixture of acetonitrile (4 mL) and NEt_3 (1 mL) in a flask and argon bubbled through the solution for 10 minutes. The flask was sealed and stirred at 70 °C for 5 h, when TLC indicated that the reaction was complete. The solvent was evaporated from the crude reaction mixture and the residue purified using flash column chromatography with progressively more polar mixtures of hexane and ethyl acetate. The product **(4)** eluted with a 1:2 mixture of hexane and ethyl acetate and was isolated as an off-white solid (0.212 g, 0.95 mmol, 73%). ^{1}H NMR (400 MHz, $CDCl_3$): δ 9.08 (s, 1H), 8.81 (s, 2H), 7.42 (d, J = 9.0 Hz, 2 H),

6.67 (d, J = 9.0 Hz, 2 H), 3.02 (s, 6 H). ^{13}C NMR (100 MHz, $CDCl_3$): δ 158.30, 156.03, 150.85, 133.17, 121.01, 111.86, 108.29, 98.33, 80.79, 40.26.

2.1.2. Synthesis of 2-(4-N,N-dimethylaminophenylethynyl)pyrimidine, (4)

2-Bromopyrimidine (0.29 g, 1.8 mmol), $PdCl_2(PPh_3)_2$ (72 mg, 0.10 mmol), CuI (39 mg, 0.20 mmol) and 4-ethynyl-N,N'-dimethylaniline (0.24, 1.7 mmol) were added to NEt_3 (11 mL) in a flask and argon bubbled through the solution for 10 minutes. The flask was sealed and stirred at room temperature overnight (16 hrs) when TLC indicated that the reaction was complete. The crude reaction mixture was diluted with ethyl acetate (100 mL) and washed successively with water and brine and dried over anhydrous sodium sulfate. The solvent was evaporated, and the crude residue was purified using flash column chromatography with progressively more polar mixtures of hexane and ethyl acetate. The product **(4)** eluted with a 1:1 mixture of hexane and ethyl acetate and was isolated as an off-white solid (0.195 g, 0.87 mmol, 53%). ^{1}H NMR (400 MHz, $CDCl_3$): δ 8.69 (d, J = 5.1 Hz, 2 H), 7.54 (d, J = 9.0 Hz, 2 H), 7.15 (t, J = 4.9 Hz, 2 H), 6.64 (d, J = 9.0 Hz, 2H), 2.99 (s, 6 H). 13C NMR (100 MHz, CDCl3): δ 157.17, 153.87, 150.92, 134.05, 118.74, 111.53, 107.31, 90.74, 87.14, 39.99.

2.2. Cocrystallization

2.2.1. Cocrystallization of 1,2-bis(5-pyrimidyl)ethyne and 5,5'-bipyrimidine with 1,3,4,5-tetrafluoro-2,6-diiodobenzene

1,2-*Bis*(5-pyrimidyl)ethyne, (**1**), (5.4 mg, 0.024 mmol) and 1,2,3,5-tetrafluoro-4,6-diiodobenzene, **1,3-DITFB,** (22.4 mg, 0.056 mmol) were weighed into a screw cap vial. Chloroform (1.5 mL) was added and the mixture vortexed until a homogeneous solution was obtained. The solvent was allowed to slowly evaporate and after 48 h block shaped crystals, (**1**)•**1,3-DITFB**, were formed. The same cocrystal formed even from a solution with a 4-fold excess of **1,3-DITFB.** The cocrystal (**2**)•**1,3-DITFB**, was similarly formed on slow evaporation of (**2**), (8.9 mg, 0.056 mmol) and **1,3-DITFB,** (47.3 mg, 0.118 mmol) and also from a solution containing a 4-fold excess of **1,3-DITFB** relative to **(2)**.

2.2.2. Cocrystallization of 2-(4-N,N-dimethylaminophenylethynyl)pyrimidine and 5-(4-N,N-dimethylaminophenylethynyl)pyrimidine with tetrafluorodiiodobenzenes

In a typical experiment, 5-(4-N,N-dimethylaminophenylethynyl)pyrimidine, (**3**), (13 mg, 0.059 mmol) and **1,3-DITFB** (24 mg, 0.060 mmol) were weighed into a screw cap vial. Chloroform (2 mL) was added and the mixture vortexed until a homogeneous solution was obtained. The solvent was allowed to slowly evaporate and after 48 h. a homogeneous mass of crystals, (**3**)•**1,3-DITFB**, were formed. The cocrystals (**4**)•**1,3-DITFB**, (**3**)•**1,2-DITFB** and (**4**)•**1,4-DITFB** were formed similarly. In

contrast, equimolar solutions of (**4**) and **1,2-DITFB** in dichloromethane, chloroform, nitromethane, acetonitrile, benzene, toluene and ethanol did not yield cocrystals suitable for single crystal X-ray analysis. A mixture of (**4**) (5.4 mg, 0.024 mmol) and **1,2-DITFB** (10.6 mg, 0.026 mmol) were weighed into a screw cap vial. Chloroform (2 mL) and benzene (1 mL) were added and the mixture vortexed until a homogeneous solution was obtained. After slow and partial evaporation of solvent, the benzene solvate cocrystal, **(4)•1,2-DITFB•benzene**, was formed. Slow evaporation of equimolar chloroform or dichloromethane solutions of (**3**) (6.5 mg, 0.029 mmol) and **1,4-DITFB** (12.2 mg, 0.030 mmol) yielded a 2:1 cocrystal 2(**3**)**•1,4-DITFB**, that was subsequently formed quantitatively from a 2:1 solution of (**3**) and **1,4-DITFB** in chloroform.

2.3. Structure Refinement

Crystal data, data collection and structure refinement details are summarized in Table 1. All H atoms were treated as riding atoms in geometrically idealized positions with C—H = 0.95 (aromatic) or 0.98 Å (methyl) and Uiso(H) = kUeq(C), where k = 1.5 for the methylene group and 1.2 for all aromatic H's. For the cocrystal **(4)•1,4-DITFB** several crystals were harvested and data collected. All these crystals were twinned. Accordingly, TwinRotMat was run through the Platon interface (Spek, 2020) providing a twinning model with a 180º rotation about the a* axis. The hklf-5 and corresponding .ins files were generated in Platon, and the structure refined as a 2-component twin with BASF converging to 0.52.

2.4. Molecular Electrostatic Potential Calculations

All molecules were geometry optimized using the Spartan molecular modelling program with DFT at the B3LYP/6-311++G** level and the corresponding molecular electrostatic potential energy surface determined using Spartan '10 software (Spartan, 2010).

3. Results and Discussion

3.1. Halogen bonded cocrystals formed with bipyrimidines as halogen bond acceptors

We were intrigued by the possibility of simple bipyrimidines functioning as tetratopic halogen bond acceptors since we had previously formed chain linked hydrogen bonded capsules on cocrystallization of resorcinarenes with bipyrimidines as tetratopic hydrogen bond acceptors (Bosch, 2007). We reasoned that 1,2,3,5-tetrafluoro-4,6-diiodobenzene would be the most compatible diiodotetrafluoro-benzene based on the similar placement of iodine and nitrogen atoms in the 6 membered rings. Accordingly we attempted to separately form cocrystals from a solution containing 2 equiv. of 1,3,4,5-tetrafluoro-2,6-diiodobenzene with each of 1,2-bis(5-pyrimidyl)ethyne and 5,5'-bipyrimidine with the expectation that each nitrogen atom would act as a halogen bond acceptor. In each

cocrystallization, however, the large clear block shaped crystals that formed comprised a 1:1 ratio of components.

The cocrystal (**1**)•**1,3-DITFB** crystalized in the monoclinic space group C2/c with one molecule of each component in the asymmetric unit as shown in Fig. 2.

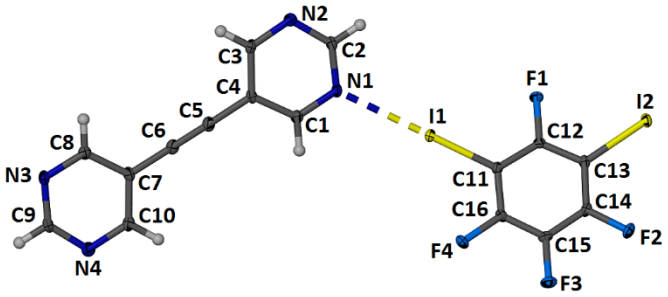

Figure 2 Asymmetric unit of the cocrystal (**1**)•**1,3-DITFB** showing atom labelling with displacement ellipsoids drawn at the 50% level for non-hydrogen atoms and hydrogen atoms shown as spheres of arbitrary size. The halogen bond is shown as a dashed line.

The bipyridine is a ditopic halogen bond donor with one N from each pyrimidine ring serving as halogen bond acceptor as shown in Figure 3(a). The nitrogen iodine distances N1---I1 and N3^{i}---I2 are 2.9105 (19) A and 2.929 (2) Å [symmetry code: (i) x+1/2, -y+3/2, z-1/2] respectively, with C-I---N angles of 173.13(8) and 172.89(7)° forming an extended zig-zag halogen bonded supramolecular polymer. The bipyrimidine is planar with a dihedral angle of 2.29(16)° between the pyrimidines. In contrast, the halobenzene is slightly twisted with respect to the halogen bonded pyrimidine with a dihedral angle of 24.04(12)°. Cooperative C-H---N hydrogen bonds connect adjacent bipyrimidines that lie in the same plane resulting in an almost planar 2-dimensional network with the perhalo benzene ring slightly tilted with respect to the plane as shown in Fig. 3(b).

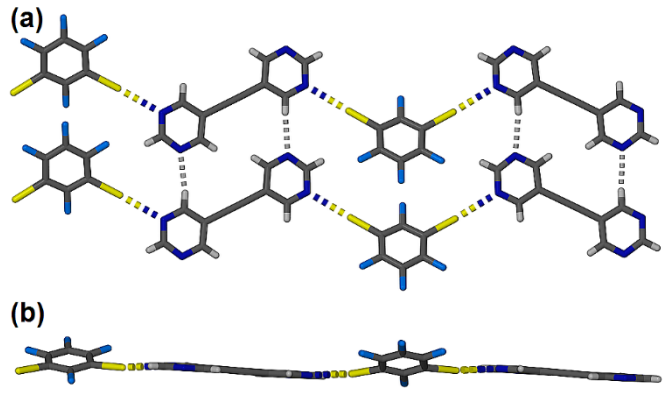

Figure 3 (a) Portion of the supramolecular polymer **(1)•1,3-DITFB** with halogen bonds shown as colored dashed lines and the weak C-H---N interactions shown as gray dashed lines. (b) Orthogonal view of the partial structure shown in (a).

The 1:1 cocrystal **(2)•1,3-DITFB**, formed from a 1:2 solution of (**2**) and **1,3-DITFB** in chloroform, crystallized in the monoclinic space group $P2_1/c$ and the asymmetric unit contains one molecule of each component as shown in Fig. 4.

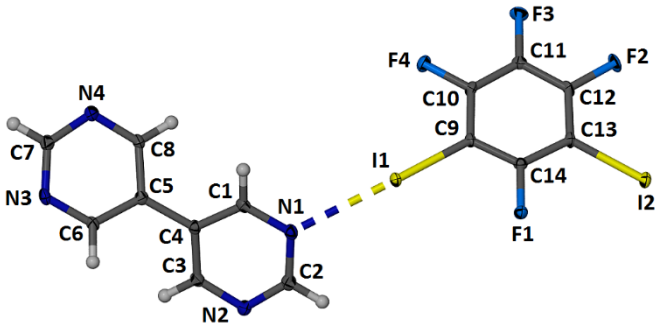

Figure 4 Asymmetric unit of the cocrystal (**2**)**•1,3-DITFB** showing atom labelling with displacement ellipsoids drawn at the 50% level for non-hydrogen atoms and hydrogen atoms shown as spheres of arbitrary size.

The structure features two unique halogen bonds that form a similar zig-zag halogen-bonded motif as shown in Fig. 5(a). The N---I distances are 2.863(3) and 2.939(3) for I1---N1 and I2---$N3^{i}$ [symmetry code: (i) x+1, -y+1/2, z-1/2] with angles C9-I1---N1 and C11-I2---$N3^{i}$ of 170.62(12) and 160.62(15)º respectively. The three aromatic rings are twisted with respect to each other with a torsional angle of 37.78(15)º between the pyrimidine rings and torsional angles of 47.77(12) and 32.06(16)º between the halobenzene and the two pyrimidine rings. This results in the individual aromatic rings all being tilted with respect to the plane of the two-dimensional sheets formed in the structure shown in Fig. 5(b).

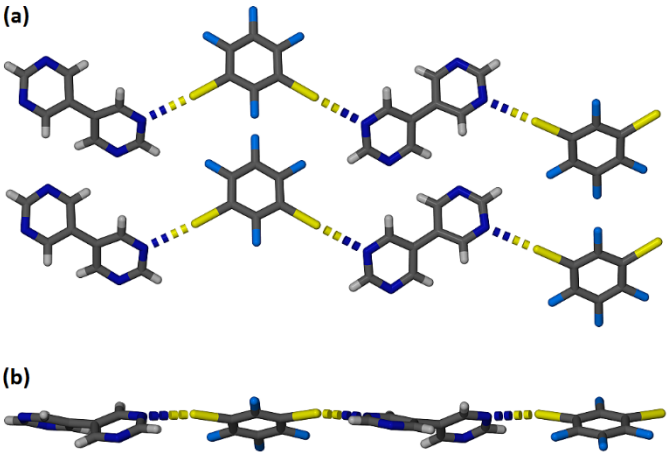

Figure 5 (a) Portion of the structure of (**2**)**•1,3-DITFB** showing the extended halogen bonded network formed with halogen bonds shown as coloured dashed lines. (b) Orthogonal view of the structure shown in (a) highlighting the twists between adjacent aromatic rings.

3.2. Activated pyrimidines as potential halogen bond acceptors

We reasoned that activated pyrimidines such as (4-N,N-dimethylaminophenylethynyl)pyrimidines would be better potential ditopic halogen bond acceptors based on our earlier studies of concomitant halogen bonding and charge transfer complexation employed in a series of related activated pyridines namely 2-,3- and 4-(4-N,N-dimethylaminophenylethynyl)pyridine (Nwachukwu, et al., 2018). In line with this expectation, molecular electrostatic potential calculations confirm that the negative electrostatic potential on the activated pyrimidine N atoms is 40 $kJmol^{-1}$ more negative than that on 1,2-(5-pyrimidyl)ethyne and similar to that on 1,2-bis(4-pyridyl)ethyne, a known ditopic halogen bond acceptor, as shown in Fig. 6.

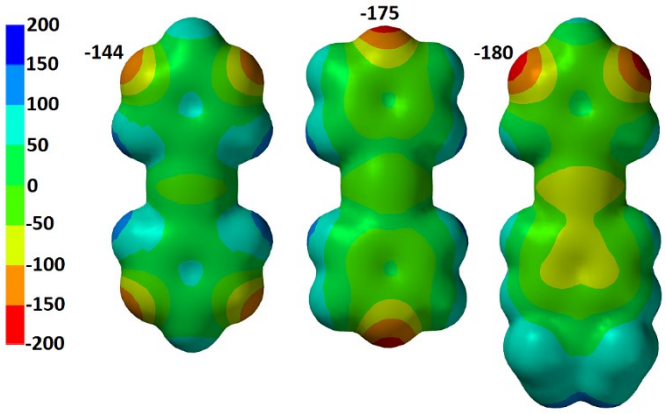

Figure 6 Molecular electrostatic potentials of 1,2-bis(5-pyrimidyl)ethyne (left), 1,2-bis(4-pyridyl)ethyne, and 5-(4-N,N-dimethylaminophenylethynyl)pyrimidine (right) shown with all values in $kJmol^{-1}$.

Accordingly, pyrimidines **(3)** and **(4)** were synthesized in good yield using the Sonogashira coupling reaction of 4-N,N-dimethylaminophenylacetylene with the appropriate halopyrimidine as shown in Fig. 1.

3.3. Cocrystals formed with activated pyrimidines (3) and (4) and diiodotetrafluorobenzenes

Each of the activated pyrimidines **(3)** and **(4)** were individually mixed with an equimolar amount of **1,3-DITFB** in chloroform and the solution allowed to slowly evaporate. Single crystals of the each of the resultant colorless 1:1 cocrystals were analyzed by X ray diffraction.

The cocrystal **(3)•1,3-DITFB** crystalized in the monoclinic space group $P2_1/m$ and the asymmetric unit included one half of each component as shown in Fig. 7.

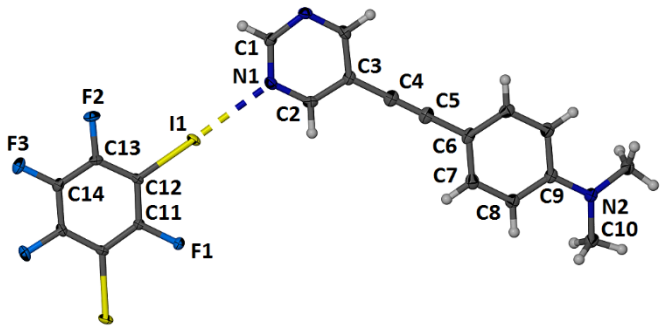

Figure 7 Asymmetric unit of the cocrystal (**3**)•**1,3-DITFB** showing atom labelling with displacement ellipsoids drawn at the 50% level for non-hydrogen atoms and hydrogen atoms shown as spheres of arbitrary size.

The unique halogen bond has a N---I distance of 2.920(2) Å and a near linear C-I---N angle of 178.27(6)˚ typical of halogen bonds. The halogen bonded components form a zig-zag ribbon in which the pyrimidines **(3)** on adjacent ribbons interdigitate as shown in Figure 8. There are several close contacts between these adjacent halogen bonded ribbons. There is a Type I F---F contact with C2-F2---F2^{i} angle of 164.25(14) and with a F2---F2^{i} separation of 2.5371 Å [symmetry code: (i) -x, -y+1, -z+2], shown as X in Fig. 8 and, the separation between one of the methyl hydrogens and F1 is close to the sum of the van der Waals radii resulting in a bifurcated C-H---F interaction, shown as y in Fig. 8.

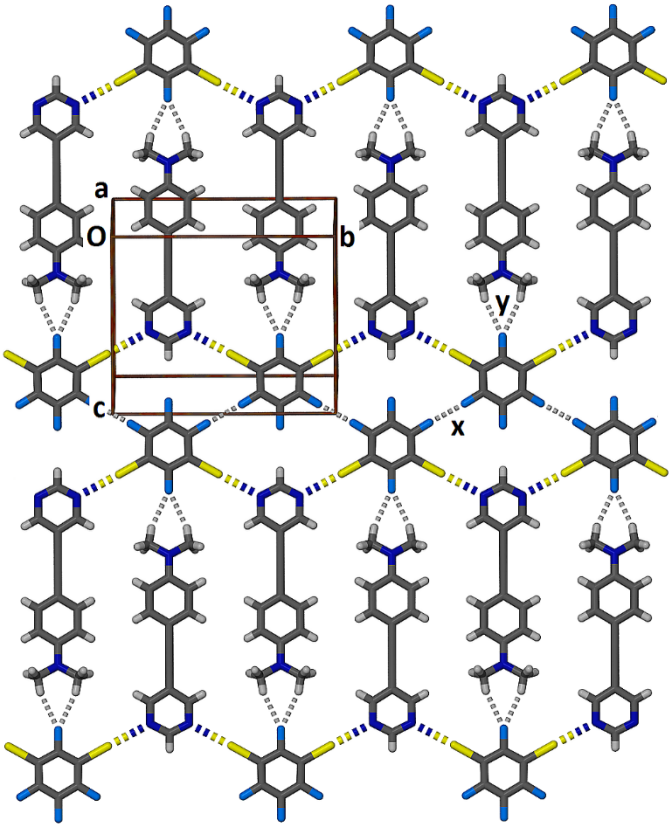

Figure 8 View of a portion of the planar sheet in the cocrystal (**3**)•**1,3-DITFB** showing the halogen bonded interactions as split colour dashed lines and the F---F and C-H---F interactions shown as grey dashed lines.

The cocrystal (**4**)•**1,3-DITFB** crystalized in the triclinic space group P-1 and the asymmetric unit includes two molecules of each component as shown in Fig. 9.

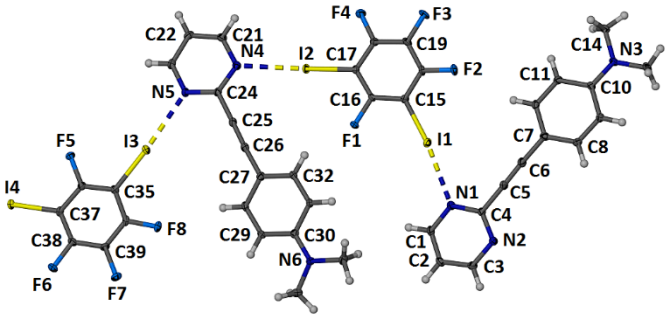

Figure 9 Asymmetric unit of the cocrystal (**4**)•**1,3-DITFB** partially labelled and displacement ellipsoids drawn at the 50% level for non-hydrogen atoms and hydrogen atoms shown as spheres of arbitrary size.

The structure features four unique halogen bonds three of which are shown in Fig. 9 and the fourth between I2 and N5^{i} [symmetry code: (i) x-2, y-1, z-1]. The N---I distances range from 2.866(2) to 2.924(2) Å and almost linear C-I---N angles between 173.54(8) and 177.96(8)˚. The two unique molecules **(4)** are essentially planar with dihedral angles between the pyrimidine and phenyl moieties of 4.62(10) and 6.93(10)º, while the dihedral angles between the pyrimidine and perhalobenzene rings are 1.60(8) and 3.64(10)º. Consequently, the entire asymmetric unit is essentially planar. The four components of the asymmetric unit form a trapezoid that close packs with multiple close C-H---F and C-H---I contacts to form planar sheets as shown in Fig. 10.

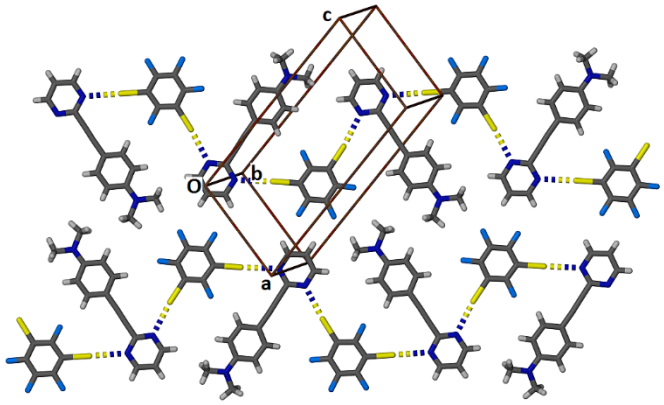

Figure 10 Partial view of the planar sheet in the cocrystal (**4**)•**1,3-DITFB**.

Given these results we attempted to co-crystallize mixtures of **(3)** or **(4)** with equimolar amounts of 1,2-diiodotetrafluorobenzene and 1,4-diiodotetrafluorobenzene, **1,2-DITFB** and **1,4-DITFB**. We were able to form 1:1 cocrystals of (**3**)•**1,2-DITFB**.suitable for X-ray analysis but were not able to form the corresponding cocrystal with pyrimidine **(4)**. The cocrystal **(3)•1,2-DITFB** crystalized in the triclinic space group P-1 with one molecule of each component in the asymmetric unit shown in Fig. 11.

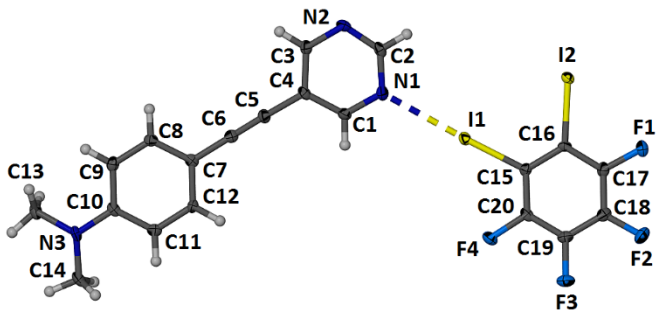

Figure 11 Asymmetric unit of the cocrystal **(3)•1,2-DITFB** with atoms labelled and displacement ellipsoids drawn at the 50% level for non-hydrogen atoms and hydrogen atoms shown as spheres of arbitrary size.

Two asymmetric units form a rhomboid halogen bonded dimeric unit with two unique halogen bonds, N1---I1 and N2^{i}---I2 that have N---I distances of 2.907(2) and 2.894(2) Å and C-I---N angles of 176.84(7) and 177.90(7)º for C15-I1---N1 and C16-I2---N2^{i} respectively [symmetry code: (i) -x+1, -y+2, -z+2]. The pyrimidine is slightly bent with a dihedral angle between the two rings of 8.06(18)º while the dihedral angle between the pyrimidine and the perhalobenzene is 9.46(18)º and the rhomboidal halogen bonded unit is almost planar and close packs with two close C-H---F contacts to form planar 2D sheets as shown in Fig. 12.

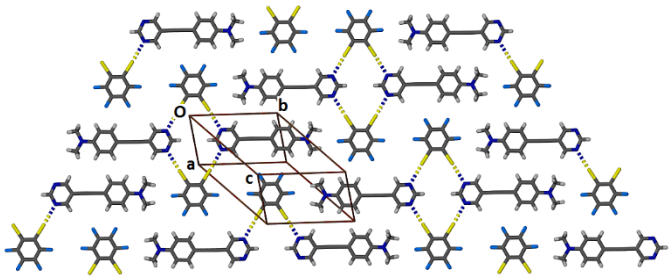

Figure 12 Partial view of the planar sheets formed in the structure of the cocrystal **(3)•1,2-DITFB**.

While all the previous cocrystals formed readily from equimolar solutions in either dichloromethane or chloroform the combination of (**4**) and 1,2-diiodotetrafluorobenzene did not result in the formation of the corresponding cocrystal. Equimolar solutions in other solvents including nitromethane, benzene, toluene and ethanol either individually or in combination with chloroform or dichloromethane were also prepared and cocrystals suitable for single crystal X-ray analysis were formed from a mixture of chloroform and benzene. The cocrystal included a benzene molecule, **(4)•1,2-DITFB•benzene**, and crystalized in the monoclinic space group P21/n with one molecule of each component in the asymmetric unit shown in Fig. 13.

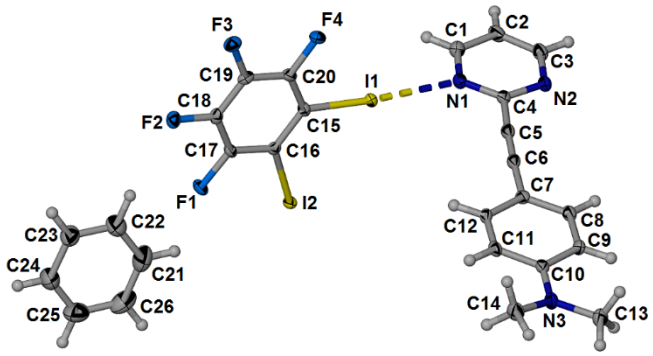

Figure 13 Asymmetric unit of the cocrystal **(4)•1,2-DITFB•benzene** with atoms labelled and displacement ellipsoids drawn at the 50% level for non-hydrogen atoms and hydrogen atoms shown as spheres of arbitrary size.

There are two unique halogen bonds with N---I distances of 2.892(3) and 2.955(3) Å for N1---I1 and $N2^{i}$---I2 respectively and C-I---N angles of 175.33(11) and 172.47(11)º for C15-I1---N1 and C16-I2---$N2^{i}$ respectively [symmetry code: (i) x+1/2, -y+3/2, z+1/2]. It is however noteworthy that the pyrimidine and halobenzene rings are almost orthogonal with a dihedral angle of 81.57(10)º and while a one-dimensional halogen bonded network is formed with the cocrystal, this cocrystal differs from all the others in that it is nonplanar. The twisted nature of the halogen bonded network is highlighted in the two views shown in Fig. 14. The view along the a-axis in Fig. 15 demonstrates the role of the solvent benzene in facilitating the formation of a three-dimensional structure.

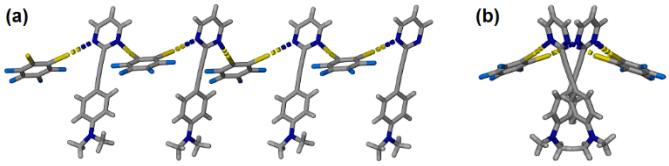

Figure 14 Two mutually orthogonal views of the twisted halogen bonded strand of alternating molecules **(4)** and **1,2-DITFB** within the cocrystal **(4)•1,2-DITFB•benzene**.

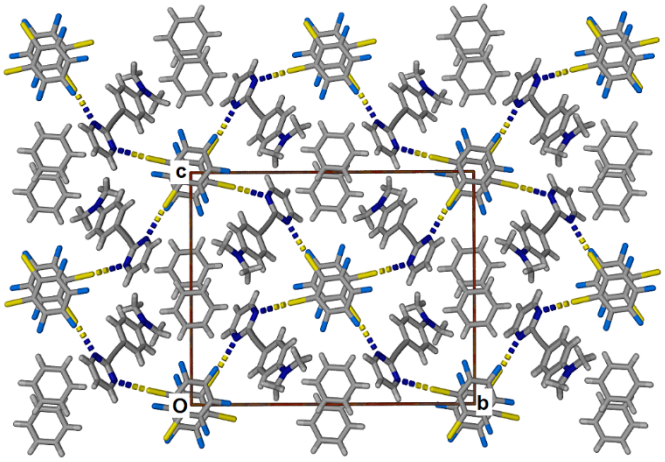

Figure 15 View of the cocrystal **(4)•1,2-DITFB•benzene** along the a-axis.

In contrast, slow evaporation of an equimolar solution of (**4**) and 1,4-diiodotetrafluorobenzene in chloroform yielded a crystalline solid suitable for single crystal X-ray analysis. The cocrystal, **(4)•1,4-DITFB**, crystallized in the monoclinic space group P21/c and the asymmetric unit contained one molecule of each of the components as shown in Fig. 16.

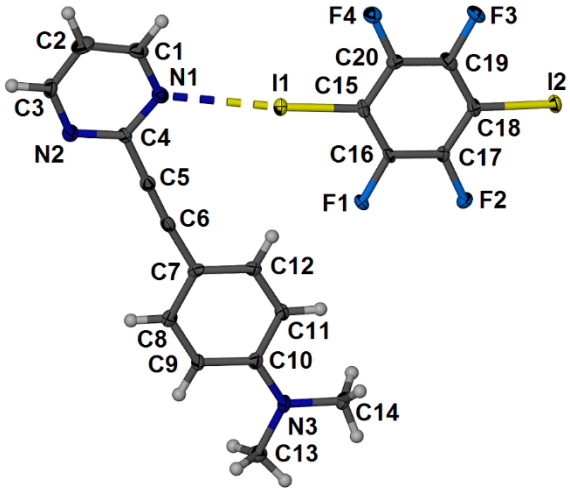

Figure 16 Asymmetric unit of the cocrystal **(4)•1,4-DITFB** with atoms labelled and displacement ellipsoids drawn at the 50% level for non-hydrogen atoms and hydrogen atoms shown as spheres of arbitrary size.

There are two unique halogen bonds with N---I distances of 3.028(8) and 2.956(8)Å for N1---I1 and $N2^{i}$---I2 and C-I---N angles of 174.7(3) and 176.7(3)º for C15-I1---N1 and C18-I2---$N2^{i}$ respectively [symmetry code: (i) -x+1, ½+y, 3/2-z]. The pyrimidine **(4)** is essentially planar with a dihedral angle of 2.9(6)º between the pyrimidine and phenyl rings while the perhalobenzene is slightly twisted with respect to the pyrimidine ring with a dihedral angle of 15.3(6)º. In the extended structures alternating pyrimidines are flipped thereby generating linear strands of **(4)•1,4-DITFB** that interdigitate to form a planar supramolecular network shown in Fig. 17.

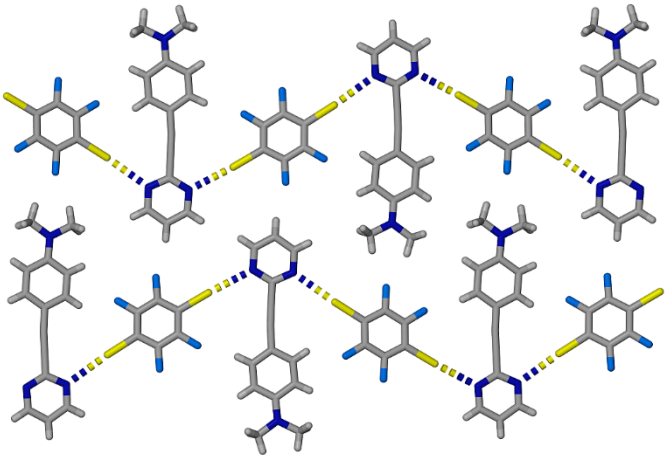

Figure 17 Partial view of plane formed in the structure of **(4)•1,4-DITFB** with atoms labelled and displacement ellipsoids drawn at the 50% level for non-hydrogen atoms and hydrogen atoms shown as spheres of arbitrary size.

Interestingly the cocrystal from a dichloromethane solution of (**3**) and 1,4-diiodotetrafluorobenzene was found to be a 2:1 cocrystal. The cocrystal was subsequently formed directly from a 2:1 mixture of **(3)** and 1,4-diiodotetrafluorobenzene and **2(3)•1,4-DITFB** crystalized in the triclinic space group P-1. The asymmetric unit contained one pyrimidine (**1**) and one half of the **1,4-DITFB** as shown in Fig. 18.

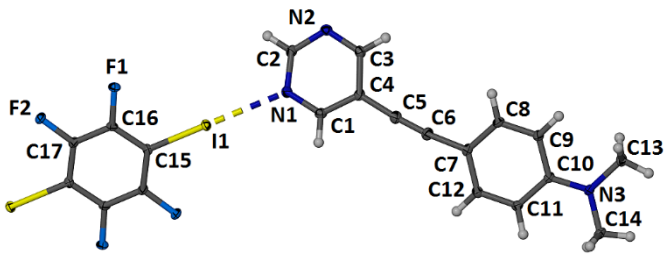

Figure 18 Asymmetric unit of the cocrystal **2(3)•1,4-DITFB** with atoms labelled and displacement ellipsoids drawn at the 50% level for non-hydrogen atoms and hydrogen atoms shown as spheres of arbitrary size.

The unique halogen bond has a N---I distance of 2.8648(13)Å with a C-I---N angle 176.16(5)º. The pyrimidine **(3)** is slightly bent and twisted with a dihedral angle of 15.81(8)º between the pyrimidine and aminophenyl rings while the perhalobenzene is also twisted with respect to the pyrimidine ring with a dihedral angle of 15.81(8)º. The 2:1 halogen bonded complex's pack side-by-side as shown in Fig. 19 with adjacent pyrimidines forming a C-H---N hydrogen bond that has C---N distance of 3.418(2) Å.

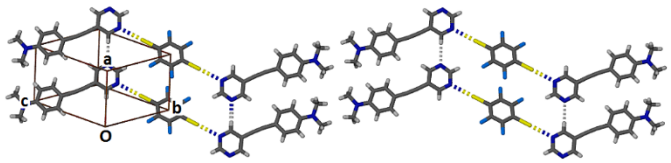

Figure 19 Partial view of the packing of discreet **2(3)•1,4-DITFB** complexes with the halogen bonds shown with dashed lines with split colours and C-H---N interactions shown with narrow grey dashed lines.

The N--I halogen bond distances of all the cocrystals reported range from 2.863 to 2.939 Å corresponding to a range of 81.1 to 83.3 % of the sum of the van der Waals radii (Bondi, 1968) and the bond angles are above 170º, with one exception, in accordance with the expected linear nature of the halogen bond. To put these values in context it should be noted that the N---I bond distance in the cocrystal formed between pentafluoroiodobenzene and the strongly basic pyridine, 4-(N,N-dimethylaminopyridine, is reported as 2.863Å (Prasang, el al., 2009) and the N---I bond distance in the cocrystal formed between pentafluoroiodobenzene and 3,5-dimethylpyridine is 2.831Å (Wasilewska, et al., 2007).

In summary we have demonstrated that pyrimidines are viable halogen bond acceptors and that activated pyrimidines can reliably act as effective ditopic halogen bond acceptors.

References

Barbour, L. J. (2001) *J. Supramol. Chem.* **1**, 189−191.

Barnes, C. L. & Bosch, E. (2005) *Cryst. Growth Des.,* **15***,* 1049-1053.

Bosch, E. (2007) *CrystEngComm,* **9**, 191-198.

Bruker (2016). APEX2, SAINT, SADABS, Bruker AXS Inc., Madison, Wisconsin, USA.

Bruno, I. J., Cole, J. C., Edgington, P. R., Kessler, M., Macrae, C. F., McCabe, P., Pearson, J. & Taylor, R. (2002) *Acta Cryst.* **B58**, 389-397.

Cavallo, G., Metrangolo, P., Milan,i R., Pilati, T.; Priimagi, A., Resnati, G. & Terraneo, G. (2016) *Chem. Rev*., **116**, 2478-2601.

Georgiev, I., Barnes, C. L., Draganjac, M. & Bosch E. (2004) *Cryst. Growth Des.,* **4***,* 235-239.

Gilday, L. C., Robinson, S. W., Barendt, T. A., Langton, M. J., Mullaney, B. R. & Beer, P. D. (2015) *Chem. Rev.,* **115**, 7118-7195.

Groom, C. R., Bruno, I. J., Lightfoot M. P. & Ward, S. C. (2016) *Acta Cryst.* **B72***,* 171-179.

Ji, B., Wang, W., Deng, D. & Zhang Y. (2011) *Cryst. Growth Des.,* **11***,* 3622-3628.

Ji, B., Wang, W., Deng, D., Zhang Y., Cao, L., Zhou, L., Ruan, C. & Li, T. (2013) *CrystEngComm,* **15**, 769-774.

Nwachukwu, C. I., Kehoe, Z. R., Bowling, N. P., Speetzen, E. D. & Bosch, E. (2018) *New J. Chem.* **42**, 10615-10622.

Sheldrick, G. M. (2015) *Acta Cryst.* **A71**, 3-8.

Sheldrick, G. M. (2015) *Acta Cryst.* **C71**, 3-8.

Spartan (2010) Spartan ’10 by Wavefunction.

Spek, A. L. (2020) *Acta Cryst.* **E76***,* 1-11.

Van der Helm, D. (1973) *J. Cryst. Mol. Struct*. **3***,* 249–258.

Table 1 Experimental details

	(1)_eb897_a	(2)_eb843_a	(3)_eb797_a	(4)_eb814_a
Crystal data				
Chemical formula	$C_{10}H_6N_4 \cdot C_6F_4I_2$	$C_8H_6N_4 \cdot C_6F_4I_2$	$C_{14}H_{13}N_3 \cdot C_6F_4I_2$	$2(C_{14}H_{13}N_3) \cdot 2(C_6F_4I_2)$
M_r	584.05	560.03	625.13	1250.27
Crystal system, space group	Monoclinic, $C2/c$	Monoclinic, $P2_1/c$	Monoclinic, $P2_1/m$	Triclinic, $P\bar{1}$
a, b, c (Å)	27.2812 (12), 6.2100 (3), 20.9742 (9)	10.4617 (10), 6.4681 (6), 23.966 (2)	6.9939 (5), 13.640 (1), 11.2299 (8)	9.1740 (7), 14.0178 (10), 17.5605 (13)
α, β, γ (°)	90, 106.931 (1), 90	90, 100.069 (1), 90	90, 94.260 (1), 90	100.065 (1), 95.285 (1), 107.225 (1)
V (Å^3)	3399.4 (3)	1596.7 (3)	1068.34 (13)	2098.8 (3)
Z	8	4	2	2
μ (mm^{-1})	3.75	3.99	2.99	3.04
Crystal size (mm)	0.2 × 0.1 × 0.03	0.44 × 0.23 × 0.09	0.25 × 0.20 × 0.10	0.50 × 0.27 × 0.17
Data collection				
Absorption correction	Multi-scan *SADABS* V2014 (Bruker)	Multi-scan *SADABS* V2014 (Bruker)	Multi-scan *SADABS* V2014(Bruker)	Multi-scan *SADABS* V2014(Bruker)
T_{min}, T_{max}	0.700, 1.000	0.649, 1.000	0.860, 1.000	0.806, 1.000
No. of measured, independent and observed [$I > 2\sigma(I)$] reflections	19984, 3766, 3544	18558, 3557, 3283	13568, 2445, 2326	26355, 9224, 8375
R_{int}	0.026	0.039	0.015	0.024
$(\sin \theta/\lambda)_{max}$ (Å^{-1})	0.643	0.643	0.640	0.641
Refinement				

$R[F^2 > 2\sigma(F^2)]$, $wR(F^2)$, S	0.020, 0.050, 1.08	0.029, 0.051, 1.18	0.018, 0.043, 1.06	0.021, 0.050, 1.04
No. of reflections	3766	3557	2445	9224
No. of parameters	235	217	149	527
$\Delta\rho_{max}$, $\Delta\rho_{min}$ (e Å^{-3})	1.22, −0.46	0.94, −1.00	1.12, −0.56	0.99, −0.46

Computer programs: *SMART* (Bruker, 2014), *SAINT* (Bruker, 2014), SHELXT 2018/2 (Sheldrick, 2015a), *SHELXL2018*/3 (Sheldrick, 2015b), *X-SEED* (Barbour, 2001).

Table 2 Experimental details

	(5)_eb948_a	(6)_eb951_a_F	(7)_eb945_a_tw
Crystal data			
Chemical formula	$C_{14}H_{13}N_3 \cdot C_6F_4I_2$	$C_{14}H_{13}N_3 \cdot C_6F_4I_2 \cdot C_6H_6$	$C_{14}H_{13}N_3 \cdot C_6F_4I_2$
M_r	625.13	703.24	625.13
Crystal system, space group	Triclinic, $P\overline{1}$	Monoclinic, $P2_1/n$	Monoclinic, $P2_1/c$
a, b, c (Å)	9.3688 (6), 11.4346 (7), 12.0797 (7)	7.2512 (6), 20.6215 (17), 17.1906 (14)	9.0191 (18), 26.805 (5), 9.5664 (19)
α, β, γ (°)	62.075 (1), 82.310 (1), 68.234 (1)	90, 101.166 (1), 90	90, 112.052 (3), 90
V (Å^3)	1060.63 (11)	2521.9 (4)	2143.6 (7)
Z	2	4	4
μ (mm^{-1})	3.01	2.54	2.98
Crystal size (mm)	0.38 × 0.18 × 0.10	0.40 × 0.25 × 0.04	0.33 × 0.32 × 0.12
Data collection			
T_{min}, T_{max}	0.727, 1.000	0.909, 1.000	0.756, 1.000
No. of measured, independent and observed [$I > 2\sigma(I)$] reflections	13784, 4679, 4312	28632, 5618, 4701	4793, 4793, 4305
R_{int}	0.014	0.044	?
$(\sin \theta/\lambda)_{max}$ (Å^{-1})	0.641	0.643	0.647
Refinement			
$R[F^2 > 2\sigma(F^2)]$, $wR(F^2)$, S	0.020, 0.046, 1.10	0.032, 0.078, 1.05	0.056, 0.147, 1.13
No. of reflections	4679	5618	4793
No. of parameters	264	318	265
$\Delta\rho_{max}$, $\Delta\rho_{min}$ (e Å^{-3})	1.44, −0.61	1.93, −0.44	3.63, −3.33

Computer programs: Bruker *SMART*, Bruker *SAINT*, SHELXT 2018/2 (Sheldrick, 2015a), *SHELXL2018*/3 (Sheldrick, 2015b), *X-SEED* (Barbour, 2001)